



# Preparation of mesoporous silica with grafted chelating agents for uptake of metal ions

Zeid A. Allothman<sup>a,\*</sup>, Allen W. Apblett<sup>b</sup>

<sup>a</sup> Department of Chemistry, College of Science Building #5, PO Box 2455, King Saud University, Riyadh 11451, Saudi Arabia

<sup>b</sup> Department of Chemistry, Oklahoma State University, 107 Physical Sciences, Stillwater, OK, USA

## ARTICLE INFO

### Article history:

Received 13 May 2009

Received in revised form 6 September 2009

Accepted 19 September 2009

### Keywords:

Mesoporous silica

TEOS

GPTMS

<sup>29</sup>Si NMR

Copper

## ABSTRACT

Functionalized hexagonal mesoporous silicas were prepared by chemical modification of a surfactant free mesoporous silica (OSU-6-W) with 3-glycidoxypropyltrimethoxysilane. Different degrees of derivitization with 3-glycidoxypropyl were realized by using either a single silylation reaction or two silylation reactions with an intermediate hydrolysis step. The two resulting inorganic–organic hybrids were characterized by solid-state <sup>29</sup>Si nuclear magnetic resonance (NMR) spectroscopy, a titration method, and elemental analysis of the modified samples and the average numbers of pendant groups were found to be 2.17 and 3.49 groups/nm<sup>2</sup>, respectively. Surface area analysis showed that these materials have pore diameters of 40.7 and 33.2 Å and surface areas of 966 and 720 m<sup>2</sup>/g, respectively. Infrared spectroscopy, solid-state NMR for <sup>13</sup>C and <sup>29</sup>Si nuclei and X-ray diffraction patterns are in agreement with the success of the preparation of organically modified mesoporous silicas. The basic centers of the attached pendant groups provide the capacity to extract copper from aqueous solution via an adsorption process that followed the Langmuir model and had a remarkably high capacity of 6.75 mmol g<sup>-1</sup> for adsorption of copper.

© 2009 Elsevier B.V. All rights reserved.

## 1. Introduction

The covalent grafting of organic molecules with desired functions onto a variety of inorganic surfaces has significant practical advantages, such as improved structural and thermal stability, swelling behavior, accessibility to the reactive centers, and insolubility in organic and aqueous solvents [1,2]. One example of such materials is inorganic–organic hybrids based on porous inorganic substrates with pendant metal-coordinating groups that provide green chemical solutions in the areas of catalysis and removal of contaminants [3,4]. Among the many inorganic materials that are capable of covalently binding organic compounds, mesoporous silica materials are extremely promising due to their exceptionally high surface area, large pores, and high thermal and chemical stabilities [1,4]. The presence of high concentrations of silanol (Si–OH) groups on the surface of mesoporous silicas enables the immobilization of a great number of organic molecules [5]. Furthermore, a large family of different mesoporous silicate structures can be synthesized through the variation of reaction conditions and the nature of the templating molecules or ion used [6].

Materials containing glycidyl functional groups have proven extremely popular for the attachment of various reactive groups and ligands due to the facile nucleophilic ring-opening reaction of the pendant epoxide functionality [7]. Amines react to yield materials with favorable exchange kinetics for transition metal ions, due to the hydrophilic character of the resultant material that is the result of the ring-opening reaction which generates a hydroxyl group on the carbon atom β to the incoming amine [8]. This group makes this site rather hydrophilic, and is believed to make these materials particularly effective in applications involving the treatment of aqueous feed streams for metal-ion recovery. It is much less clear whether this hydroxyl group is able to function as an additional binding site for chelation of metals [9]. The purpose of this work was to develop a new family of mesoporous silicas with grafted chelating agents for complexing metal ions with increased functional group coverage and pore sizes that were maintained as large as possible. To realize these objectives a single grafting step with 3-glycidoxypropyltrimethoxysilane was compared to a procedure that used two silylation reactions with an intermediate hydrolysis reaction. The products were characterized using several techniques including X-ray powder diffraction (XRD), N<sub>2</sub> adsorption–desorption analysis (BET), solid-state <sup>13</sup>C and <sup>29</sup>Si MAS NMR spectroscopy, diffuse reflectance infrared Fourier transform (DRIFT) spectroscopy, UV–vis spectrometer, and elemental analysis.

\* Corresponding author. Tel.: +966 14675999; fax: +966 14675992.  
E-mail address: [zaothman@ksu.edu.sa](mailto:zaothman@ksu.edu.sa) (Z.A. Allothman).

## 2. Material and methods

### 2.1. Materials

The chemicals used in this work included: tetraethylorthosilicate (TEOS) as the silica sources and 1-hexadecylamine (HDA) [Aldrich] as the surfactant template, 1,3,5-Trimethylbenzene (mesitylene) [TCI] and dodecane [Aldrich] were used as organic additives during the mesoporous silica preparation. Cyclohexylamine and proton-sponge (1,8-bis(dimethylamino)naphthalene) [Aldrich] were used as probe molecules for hydroxyl group determination. Other chemicals included absolute ethyl alcohol [Pharmco, USA], isopropyl alcohol [HPLC-UV Grade, Pharmco, USA], 3-glycidoxypropyltrimethoxy-silane (GPTMS) [98.0% Aldrich], *N,N*-dimethylformamide (DMF), boron trifluoride diethyl etherate (BF<sub>3</sub>·OEt<sub>2</sub>), toluene (99.8% HPLC grade), dry methanol, triethylamine (TEA) [99% Aldrich], dichloromethane (99.6% Aldrich), 96% sulfuric acid, sodium carbonate (Na<sub>2</sub>CO<sub>3</sub>, 0.8 M). Water was purified by reverse osmosis and deionization before use. Molecular sieves (5A, beads, 4–8 mesh) were used to dry solvents.

### 2.2. Synthesis of mesoporous material (OSU-6-W)

The mesoporous material OSU-6 was synthesized following the reported literature procedure by Tuel and Gontier [10] with several alterations. A templating solution was prepared by dissolving 16.0 g (0.067 mol) of the neutral surfactant HDA in 65 ml (3.6 mol) of distilled H<sub>2</sub>O at room temperature in a 250-ml Erlenmeyer flask, sonicating for a few minutes and magnetically stirring for 1 h until a white homogenous suspension formed. 1.0 M of HCl was added to the first mixture until the pH of the mixture was approximately 4.5. A second solution was prepared by mixing 32.0 g (0.15 mol) of TEOS, 28 ml (0.6 mol) of ethanol and 6 ml (0.1 mol) of isopropanol in a 250-ml closed Erlenmeyer flask under magnetic stirring at room temperature for about 30 min. The two solutions were then mixed with stirring for about 30 min in a sealed 500-ml flask. Next, 9.0 ml of the auxiliary organic mesitylene was added and the reaction mixture was stirred for a further 5 min. At this point, the stirring was stopped and 100 ml of distilled water was added to the flask, and then the reaction mixture was mixed thoroughly by swirling and then left to age for 14 days at 25 °C. The resulting solid was recovered by filtration, washed with distilled water and ethanol (three times each with 100 ml) using a fine filter funnel, and was dried at room temperature under vacuum for 48 h. The yield of OSU-6 was 44.85 g (~93.5%). The removal of the organic template was performed by extraction with a hydrochloric acid/ethanol mixture. In the latter process, 1.0 g of OSU-6 was washed five times with 50 ml of a hot solution of HCl–ethanol in order to remove the organic components. The product isolated by this extraction method will be referred to as OSU-6-W throughout the remainder of the paper.

### 2.3. Activation of the materials

The OSU-6-W material was activated by refluxing 10.0 g of the mesoporous silica in 100 ml of dry toluene for 4 h under a dry atmosphere, followed by washing with 100 ml dry toluene, and drying at 80 °C under vacuum. Next, 6.0 g of the dried material was reacted with a stirred solution of 20 ml of triethylamine in 100 ml of dry toluene with 20 ml of triethylamine and stirred for approximately 1 h at room temperature. The resulting material (which will be referred to as TEA-OSU-6-W) was isolated by filtration with a fine filter funnel and was washed with dry toluene (3 × 50 ml).

### 2.4. Characterization

Solid-state <sup>13</sup>C NMR and elemental analysis were used for the characterization of the ordered mesoporous materials. Solid-state

<sup>13</sup>C CP/MAS NMR spectra were obtained with a Chemagnetics CMX-II solid-state NMR spectrometer operating at 75.694 MHz for carbon-13 and a Chemagnetics 5 mm double resonance magic-angle spinning probe. Carbon-13 cross-polarization/magic-angle spinning (CP/MAS) was carried out with a quasi-adiabatic sequence (1) using two-pulse phase modulation (TPPM) decoupling (2) at 50–75 kHz. At least 3600 scans were acquired with a delay of 1.0 s between scans. The NMR samples were packed in a 5.0 mm zirconia rotor that was spun at a speed of 6.0 kHz that was maintained to within a range of ±5.0 Hz or less with a Chemagnetics speed controller. The quasi-adiabatic cross-polarization pulse sequence used a 1.0 s pulse delay, a 1.0 ms contact time, and a 5.0 μs pulse width. The C-13 CP contact pulse of 1.0 ms length was divided into 11 steps of equal length with ascending radiofrequency field strength, while the H-1 contact pulse had constant radiofrequency field strength.

Solid-state <sup>29</sup>Si nuclear magnetic resonance (NMR) spectra were recorded on a Chemagnetics CMX-II solid-state NMR spectrometer 5 mm double resonance magic-angle spinning probe operating at resonance frequencies of 59.79 MHz for <sup>29</sup>Si nucleus and the chemical shifts are given in ppm from external tetramethylsilane. The <sup>29</sup>Si CP/MAS spectra were acquired utilizing a quasi-adiabatic cross-polarization pulse sequence using a 5.0 s pulse delay, a 9.0 ms contact time, a 7.0 μs pulse width and at least 3000 scans. Proton decoupling was used during acquisition.

The diffuse reflectance infrared Fourier transform spectra were recorded on a Nicolet Magna 750 FT-IR. The spectra were collected for all samples in the range from 400 to 4000 cm<sup>-1</sup>. The samples were finely ground with approximately four times their volume of potassium bromide and the packed in a conical DRIFTS cell.

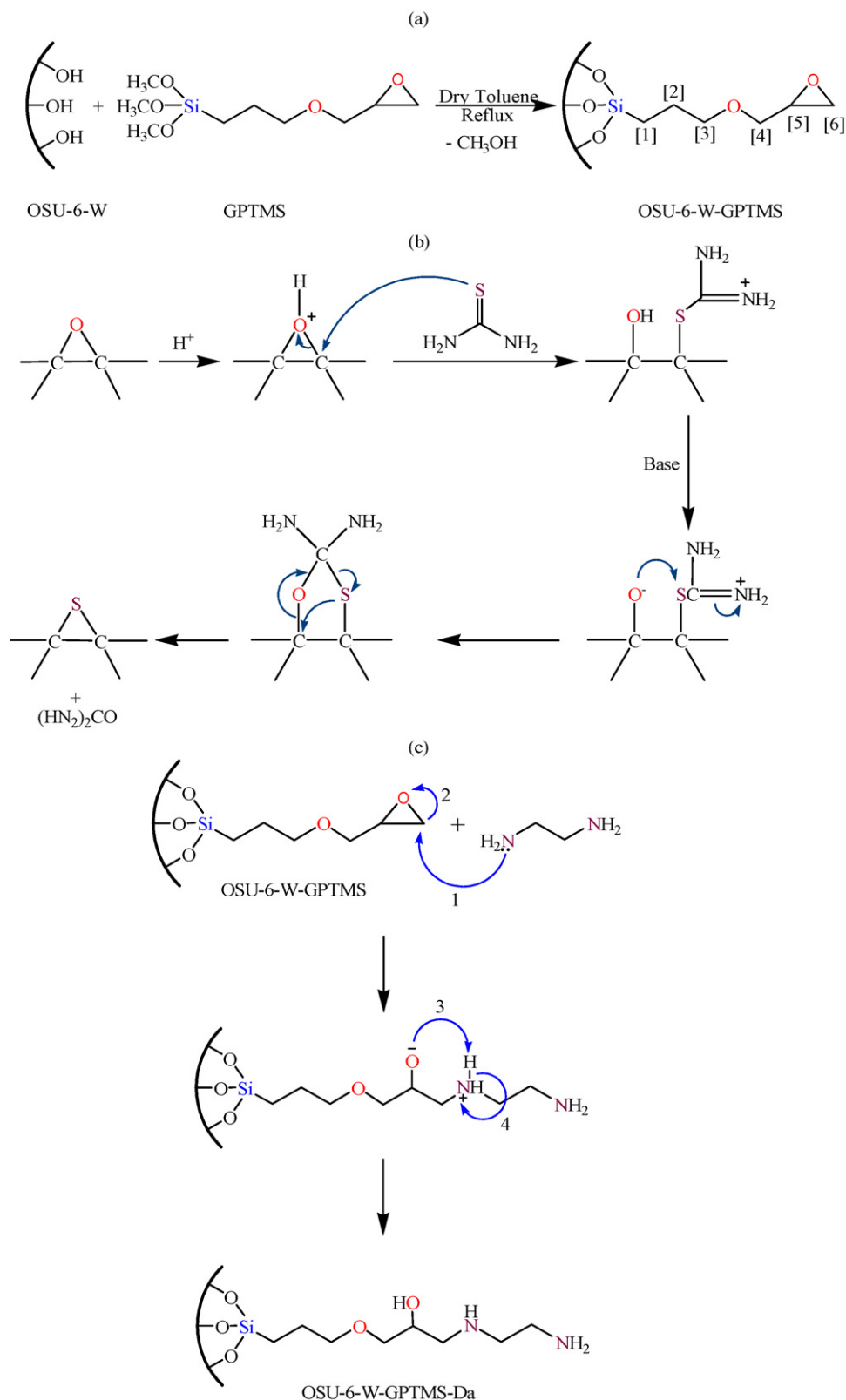
Elemental analysis for C and N was used to determine the amount of functional groups in the samples and was carried out on a LECO TruSpec Carbon and Nitrogen Analyzer. All the adsorption measurements were obtained using a UV–vis spectrophotometer or inductively coupled plasma atomic emission spectroscopy. UV–vis spectra were recorded on a PerkinElmer (Lambda EZ 201) spectrometer in the range from 200 to 800 nm, while the ICP analysis was performed on a Spectro CIROS ICP Spectrometer. The scanning electron microscopy (SEM) images of typical samples were obtained with a JEOL 640 instrument. Samples were gold coated using an Instrumental Scientific Instrument PS-2 coating unit. The SEM pictures were developed on photographic paper. Transmission electron microscopy (TEM) was performed using a JEOL 3010 electron microscope operated at 300 kV. Samples for TEM were prepared by placing droplets of a suspension of the sample in acetone on a polymer microgrid supported on a Cu grid.

### 2.5. Grafting of functional groups

3-Glycidoxypropyl-functional group was chemically attached to the as-prepared mesoporous OSU-6-W material surfaces by means of a grafting method. Two synthetic procedures were applied which are based on a combination of different synthetic methods.

#### 2.5.1. One step reaction

Mesoporous silica-supported glycidoxypropyl groups (OSU-6-W-GPTMS-1) was prepared by refluxing 3.0 g (~50 mmol) of the activated mesoporous silica (TEA-OSU-6-W) with 12.0 ml (~50 mmol) of 3-glycidoxypropyltrimethoxysilane (GPTMS) in 100 ml of dry toluene in a 250 ml round-bottom flask for 48 h under a dry atmosphere. An illustration of the reaction is schematically presented in Scheme 1. The resulting solid mixture was filtered off with a fine filter funnel, washed three times (3 × 50 ml) with toluene and then ethanol, to rinse away any surplus GPTMS. The



**Scheme 1.** The reaction scheme between GPTMS and silanol groups on the OSU-6-W surface. The final product has numbers that illustrate carbon atoms positions.

white solid was dried at 80 °C under vacuum for 24 h to give a yield 4.74 g. IR ( $\text{cm}^{-1}$ ) (KBr): 3737(m), 3660(m, br), 3237(s, br), 2991(m), 2957(s, sh), 2893(m), 2853(m), 1630(m, sh), 1463(m, sh), 1372(w), 1266(s, sh), 1224(s, br), 1148(s, br), 1061(s, br), 946(s), 808(s), 666(w), 574(w), and 490(w).

### 2.5.2. Three steps modification procedure

Second glycidyoxypropyl functionalized mesoporous silica (OSU-6-W-GPTMS-2) was prepared using two silylation steps similar to that described above. In between the two silylation steps the material was stirred with 50 ml of distilled water for 5 h, to hydrolyze

**Table 1**

Textural properties determined from nitrogen adsorption–desorption experiments at 77 K and powder XRD measurements.

Sample	Specific surface area (m <sup>2</sup> /g)	Total pore volume (cm <sup>3</sup> /g)	Average pore size (Å)	<i>d</i> <sub>100</sub> (Å)	Wall thickness (Å)
OSU-6-W	1283	1.24	51.1	62.4	21.0
OSU-6-W-GPTMS-1	966	0.92	40.7	54.6	22.4
OSU-6-W-GPTMS-2	720	0.58	33.2	51.2	25.9

any residual silicon alkoxide groups left from the first step. The product was dried at 80 °C under vacuum for 24 h to give a final yield of 5.98 g of white solid. IR (cm<sup>-1</sup>) (KBr): 3628(m, br), 3376(m), 3295(m), 2923(s, sh), 2854(s, sh), 1456(m, sh), 1351(vw), 1249(s, sh), 1138(s, br), 1077(s, br), 969(m), 797(m, sh), 679(m), 575(m), and 499(m).

### 3. Results and discussion

GPTMS is exceptional among silanes used to prepare bonded phases in the sense that the oxirane ring is highly reactive [11]. However, functionalization with this reagent can be accompanied by formation of a variety of by-products whose generation is highly pH and temperature dependent. All of the by-products may be expected to be less hydrophilic. The complexity of the bonding reaction may be responsible for the differences in ionic and hydrophobic interactions among diol phases produced under varying conditions [12]. Hydrophobic interactions arise from the hydrocarbon spacer groups with the number of hydroxy groups playing a significant role in hydrophilicity [13]. Previously the functionalization reaction was studied in detail and the amount of bonded oxiranes, vicinal diols, total hydroxy and CH contents were determined as a function of temperature, pH and time [14]. The aim was to find conditions giving the maximum surface coverage of oxirane groups on silica.

The new grafting procedure used herein utilized conditions whereby hydrolysis of the silicon alkoxides during the grafting procedure was avoided as much as possible by maintaining a strictly dry atmosphere during the silanization step. This prevented polymerization of the silyl reagent via formation of silicon-oxygen linkages and promoted the maximum coverage of the surface with the immobilized glycidoxypropyl functional groups. After silanization, the remaining alkoxides groups on silica were removed by hydrolysis during a water wash causing a concomitant condensation reaction between adjacent grafted silyl groups that creates an Ormosil polymer grafted to the mesoporous silica surface. Following this procedure with a second silanization step enhances the maximum surface density of silanes by at least 30% [15].

#### 3.1. Identification of textural properties

##### 3.1.1. X-ray powder diffraction

The pristine ordered mesoporous material, OSU-6-W, and the functionalized samples with GPTMS (OSU-6-W-GPTMS-1 and OSU-6-W-GPTMS-2) were characterized by the XRD (Fig. 1). The XRD pattern of the unmodified OSU-6-W sample, Fig. 1(A) shows three well-resolved diffraction peaks in the region of  $2\theta = 1-5^\circ$ , which can be indexed to the (100), (110), and (200) diffraction lines characteristic of the formation of well-arranged hexagonal MCM-41 mesostructures [16]. It can be noted that the (100) peak gradually shifts to higher angles with increasing amount of functional groups on the surface from OSU-6-W-GPTMS-1 to OSU-6-W-GPTMS-2, indicating an effective decrease of the pore diameters. The pore size of OSU-6-W was narrowed from ca. 51.1 Å to ca. 40.7 Å in OSU-6-W-GPTMS-1 and to ca. 33.2 Å in OSU-6-W-GPTMS-2 (Table 1). The existence of characteristic diffraction peaks in both functionalized samples indicates the long-range order of mesoporous hexagonal channels was still maintained after modification. Combination of the XRD results with the average pore diameters from surface area

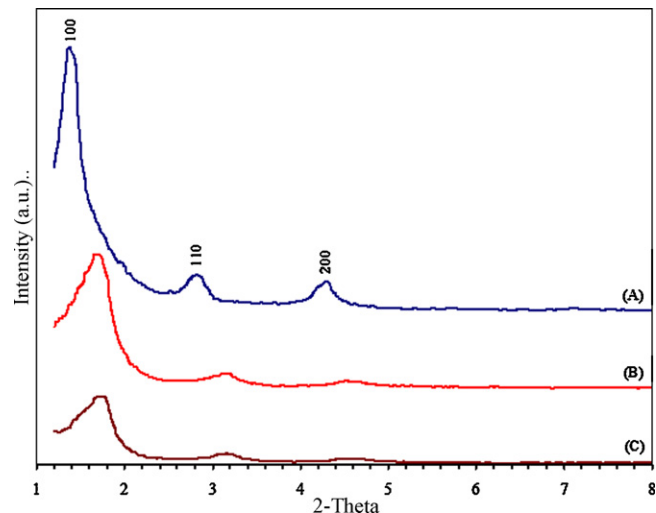


**Fig. 1.** XRD patterns in the range of 1.0–10.0° of (A) pristine ordered mesoporous material, OSU-6-W, (B) OSU-6-W-GPTMS-1, and (C) OSU-6-W-GPTMS-2. The spectra are shifted vertically for the sake of clarity.

measurements demonstrates an average thickening of the walls of about 25.9 Å in the case of OSU-6-W-GPTMS-2, which statistically would correspond to an extra one layer of Si–O–Si homogeneously spread on the original wall (20.9 Å). It also can be noticed that the *d*<sub>100</sub> peak has become broader with the increase in the loading of the functional groups, indicating a slight alteration of the ordering of the mesoporous structure as more functional groups are added to the surface.

##### 3.1.2. Nitrogen adsorption–desorption measurements

Fig. 2 shows the nitrogen adsorption–desorption isotherms for the mesoporous silicas. The textural properties of the materials

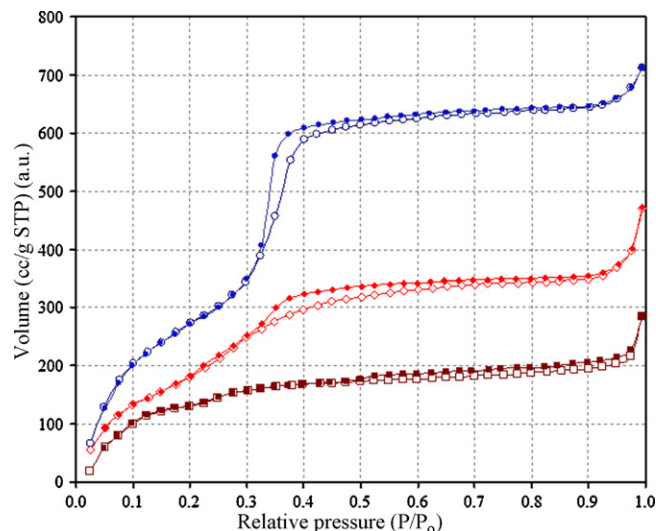


**Fig. 2.** Nitrogen adsorption–desorption isotherms of (○) OSU-6-W, (◇) OSU-6-W-GPTMS-1, and (□) OSU-6-W-GPTMS-2. Open symbols: adsorption; closed symbols: desorption. The isotherm data are shifted vertically for the sake of clarity.

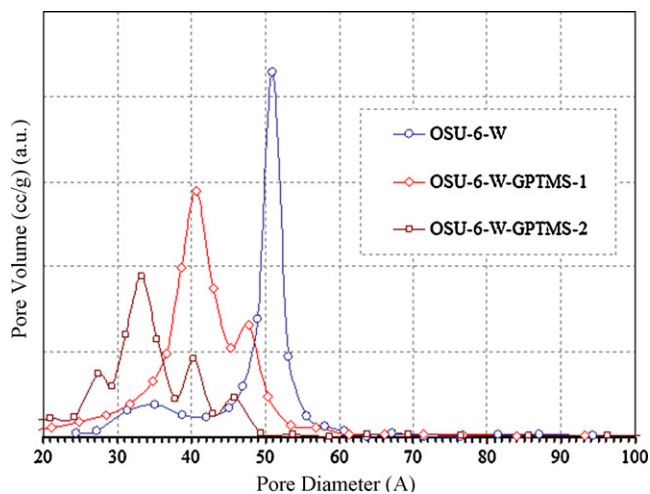


**Fig. 3.** The pore size distribution of (○) OSU-6-W (maximum at 51.1 Å), (◇) OSU-6-W-GPTMS-1 (maximum at 40.7 Å), and (□) OSU-6-W-GPTMS-2 (maximum at 33.2 Å).

are summarized in Table 1. The curves are typical for mesoporous materials with hexagonal channel arrays. After reaction with the coupling agent, the nitrogen adsorption–desorption experiments yielded a BET surface area of 966 m<sup>2</sup>/g and a total pore volume of 0.92 cm<sup>3</sup>/g for the OSU-6-W-GPTMS-1 sample, and a surface area of 720 m<sup>2</sup>/g and a total pore volume of 0.58 cm<sup>3</sup>/g for the OSU-6-W-GPTMS-2 sample. The nitrogen uptake corresponding to the filling of the mesopores has shifted to lower relative pressures indicating a reduction of the pore diameter (from 51.1 to 40.7 Å for OSU-6-W-GPTMS-1 and from 51.1 to 33.2 Å for OSU-6-W-GPTMS-2). Fig. 3 presents the pore size distribution measurements of all three samples; OSU-6-W, OSU-6-W-GPTMS-1, and OSU-6-W-GPTMS-2. It shows that for the unfunctionalized sample, OSU-6-W, the pore size distribution is a fairly narrow 3.5 Å wide. After functional-

ization with the 3-glycidoxypropyltrimethoxysilane, the pore size distributions of both functionalized samples were larger than the unfunctionalized sample. However, their pore size distributions still remain reasonably narrow at about 7.0 Å wide for both samples.

### 3.2. Characterization of morphology

#### 3.2.1. Scanning electron microscopy

The morphology, shape, and size of the particles of the mesoporous materials were characterized by high resolution scanning electron microscopy. Fig. 4(A and B) of the as-synthesized OSU-6 mesoporous silica shows a narrow particle size distribution with well defined spherical particles. Similar characteristics were observed for the mesoporous silica after extraction of the template (see Fig. 4C and D for mesoporous OSU-6-W). The particle sizes of both OSU-6 and OSU-6-W were in the range of 250–1500 nm.

#### 3.2.2. Transmission electron microscopy

The unit cell parameters obtained from the TEM images (Fig. 5) were close to those evaluated using XRD, indicating a proper calibration of electron microscopy magnification. High resolution TEM images for selected particles along [1 0 0], [1 1 1], and [1 1 0] directions correspond well with previously reported MCM-41 images.

### 3.3. Identification of the functional groups

#### 3.3.1. Solid-state <sup>29</sup>Si CP/MAS NMR spectroscopy

Solid-state <sup>29</sup>Si NMR measurements were performed in order to determine the surface structure of OSU-6-W after modification. Solid-state <sup>29</sup>Si CP/MAS NMR peak assignments were made according to those previously reported by Glaser et al. [17] for organically modified silicates (Fig. 6). The <sup>29</sup>Si CP/MAS NMR spectrum of OSU-6-W showed signals of Q<sup>4</sup> species (Si(OSi)<sub>4</sub>) at ca. −107.9 ppm, Q<sup>3</sup> species (Si(OSi)<sub>3</sub>OH) at ca. −100.4 ppm, and shoulder Q<sup>2</sup> species (Si(OSi)<sub>2</sub>(OH)<sub>2</sub>) at ca. −91.2 ppm. OSU-6-

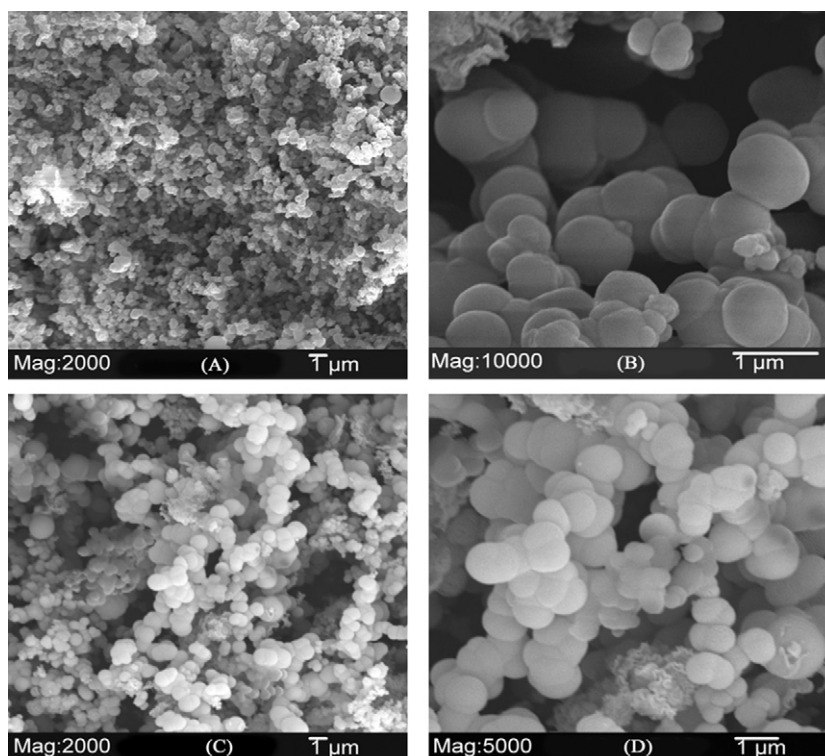


**Fig. 4.** SEM images of the as-synthesized mesoporous silica OSU-6 (A and B), HCl/EtOH washed OSU-6-W (C and D).

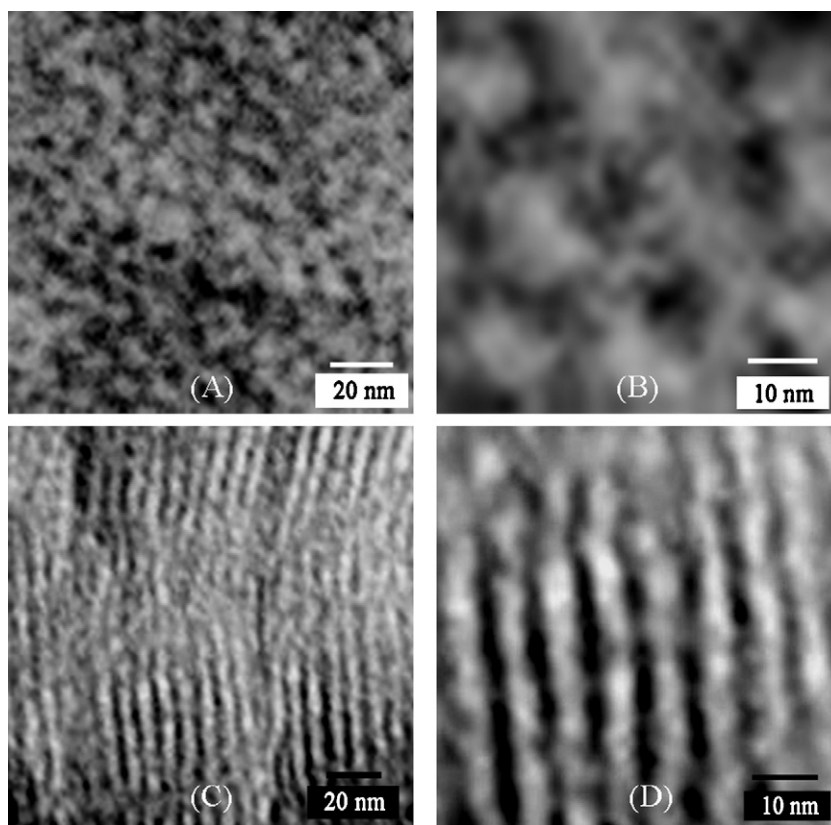


**Fig. 5.** Transmission electron microscopy images of OSU-6-W (A), (B) shows the hexagonal array (pore diameters ca. 50 Å) and (C and D) shows the pore diameter and wall thickness (wall thicknesses ca. 20 Å).

W-GPTMS-1 showed three signals at  $-48.0(T^1)$ ,  $-57.3(T^2)$ , and  $-67.1(T^3)$  ppm, while OSU-6-W-GPTMS-2 showed two signals at  $-57.2(T^2)$ ,  $-65.0(T^3)$ , corresponding to  $T^1$  ( $RSi(OSi)(OH)_2$ ),  $T^2$  ( $RSi(OSi)_2OH$ ), and  $T^3$  ( $RSi(OSi)_3$ ) groups. R here represents the alkyl group belonging to GPTMS. Besides those peaks, each modified sample also showed two peaks corresponding to  $Q^3$  and  $Q^4$  silicons. The OSU-6-W-GPTMS-1 modified sample shows relative intensity ratios for  $T^1:T^2:T^3$  close to 1.0:9.6:5.1. However, the OSU-6-W-GPTMS-2 modified sample shows relative intensity ratio for  $T^2:T^3$  close to 1.0:1.9. These NMR results reveal that the silanol groups on the OSU-6-W surfaces are highly accessible to the modification reagent, GPTMS.

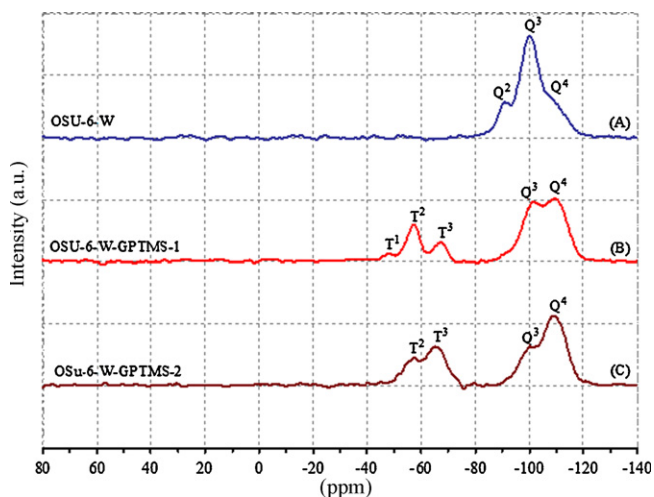


**Fig. 6.** Solid-state  $^{29}Si$  CP/MAS NMR spectra of (A) unmodified OSU-6-W, (B) OSU-6-W-GPTMS-1, and (C) OSU-6-W-GPTMS-2.

### 3.3.2. Solid-state $^{13}C$ CP/MAS NMR spectroscopy

An important feature to enrich information about the attachment of the pendant groups in the inorganic structure of the hybrid is the  $^{13}C$  NMR spectra in the solid state [1,4]. Solid-state  $^{13}C$  CP/MAS NMR peak assignments for glycidoxypropyl functional groups used in this study are based on those previously reported [18]. Two distinct peaks (Fig. 7) for the carbon atoms of the epoxy ring, of the glycidoxypropyl unit, were still observable at 42.0(C6) and 52.5(C5) ppm for OSU-6-W-GPTMS-1 sample and at 39.9(C6) and 52.2(C5) ppm for OSU-6-W-GPTMS-2 sample, indicating that most of the reactive epoxy rings were retained under the reaction conditions. Another remarkable feature was the appearance of the peak at 64.2 ppm and a broad shoulder at around 72.1 ppm, that can be assigned to either carbons of methylether and oligo- or poly(ethylene oxide) derivatives, respectively in case of OSU-6-W-GPTMS-1. These originate from the side reactions of the epoxy ring of GPTMS [19]. OSU-6-W-GPTMS-2 also displayed a peak at 56.6 ppm and one split peak at around 71.4 and 73.3 ppm, that can be assigned to either carbons of methylether and oligo- or poly(ethylene oxide) derivatives [19].

### 3.3.3. Fourier transform infrared spectroscopy (FT-IR)

Infrared spectroscopy was employed as an important tool to characterize the main products of such reactions [20]. The vibrational spectra obtained from solid samples confirmed the success of the grafting reactions, which sequence of bands are very close to those observed, when glycidoxypropyl functional groups was previously incorporated into a similar materials. The infrared spectra (Fig. 8) of OSU-6-W prior to and following grafting by 3-glycidoxypropyltrimethoxysilane (GPTMS) show several silanol bands at 3667, 3647, and 3436  $cm^{-1}$  that are not well resolved in the spectrum of OSU-6-W and OSU-6-W-GPTMS-1 also have a sharp

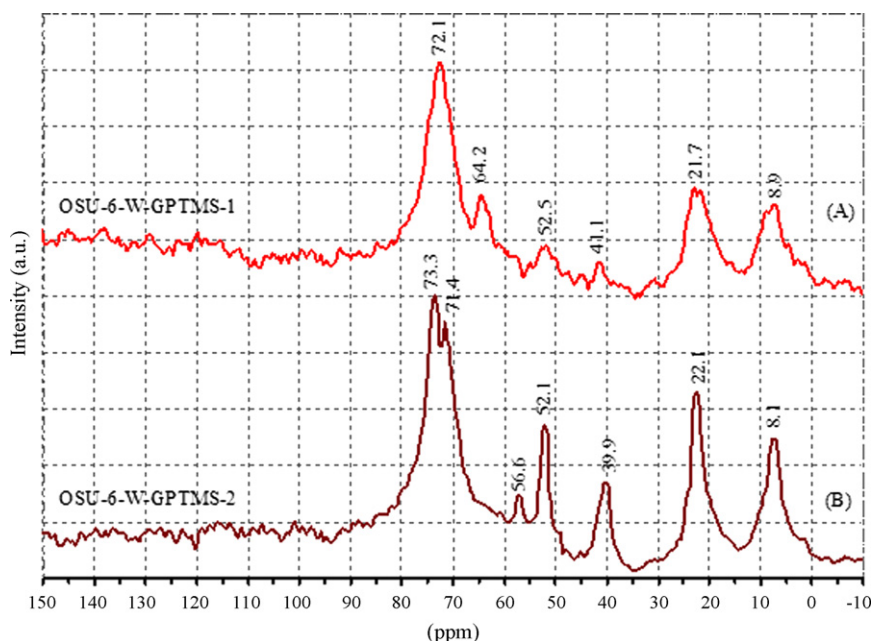


Fig. 7. Solid-state  $^{13}\text{C}$  CP/MAS NMR spectrum of (A) OSU-6-W-GPTMS-1 and (B) OSU-6-W-GPTMS-2.

absorption is observed at  $3746\text{ cm}^{-1}$  due to non-hydrogen bonded silanols [21].

In the modified sample, OSU-6-W-GPTMS-1, bands at 3740, 2955, 2886, 1462, and  $1375\text{ cm}^{-1}$  appear at the expense of the band at  $3746\text{ cm}^{-1}$ . These bands are assigned to silanol (SiO-H) stretching, C-H asymmetric stretching  $\nu_{\text{as}}(\text{CH}_2)$ , C-H symmetric stretching  $\nu_{\text{s}}(\text{CH}_2)$ ,  $\text{CH}_2$  scissor, and  $\text{CH}_3$  bending vibrations, respectively. The presence of the  $\text{CH}_3$  bending mode suggests a small amount of remaining  $-\text{OCH}_3$ . Moreover, there are bands at 3053 and  $2876\text{ cm}^{-1}$  due to the  $\nu_{\text{as}}(\text{CH}_2)$  and  $\nu_{\text{s}}(\text{CH}_2)$  vibration of the epoxy groups, respectively. The bands due to the  $\nu_{\text{as}}(\text{OC-H})$  and  $\nu_{\text{s}}(\text{OC-H})$  vibrations of the methoxy groups in GPTMS were at 2988 and  $2855\text{ cm}^{-1}$ , respectively. The bands assignable to methoxy groups confirm that the OSU-6-W-GPTMS-1 has low coverage and give indication of the possibility of adding more functional groups onto the surface. The FT-IR spectra of epoxides show characteristic bands at  $1224\text{ cm}^{-1}$  (ring breathing), and  $950\text{--}810\text{ cm}^{-1}$  (asymmetrical ring stretching) [22].

The OSU-6-W-GPTMS-2 modified sample has bands at 3628, 2946, 2880, and  $1457\text{ cm}^{-1}$  who intensity increase at the expense of the band at  $3746\text{ cm}^{-1}$  of OSU-6-W-GPTMS-1. These bands are assigned to silanol (SiO-H) stretching, C-H asymmetric stretching  $\nu_{\text{as}}(\text{CH}_2)$ , C-H symmetric stretching  $\nu_{\text{s}}(\text{CH}_2)$ , and  $\text{CH}_2$  scissor, respectively. Moreover, there are bands at 3048 and  $2871\text{ cm}^{-1}$  due to the  $\nu_{\text{as}}(\text{CH}_2)$  and  $\nu_{\text{s}}(\text{CH}_2)$  vibration of the epoxy groups, respectively. The bands due to  $\nu_{\text{as}}(\text{OC-H})$  and  $\nu_{\text{s}}(\text{OC-H})$  vibrations of methoxy groups in GPTMS were not observed. That means the OSU-6-W-GPTMS-2 has higher coverage and also gives an indication of formation of a highly ordered monolayer of the functional groups on the surface. The band positions are similar to those reported in the literature [23]. The bands in the two modified samples show shift to lower wavelength and increase in the intensities from the OSU-6-W-GPTMS-1 to OSU-6-W-GPTMS-2. These observations indicate high surface loading in the case of OSU-6-W-GPTMS-2 which has been confirmed by the solid-state  $^{29}\text{Si}$  and  $^{13}\text{C}$  NMR and elemental analysis.

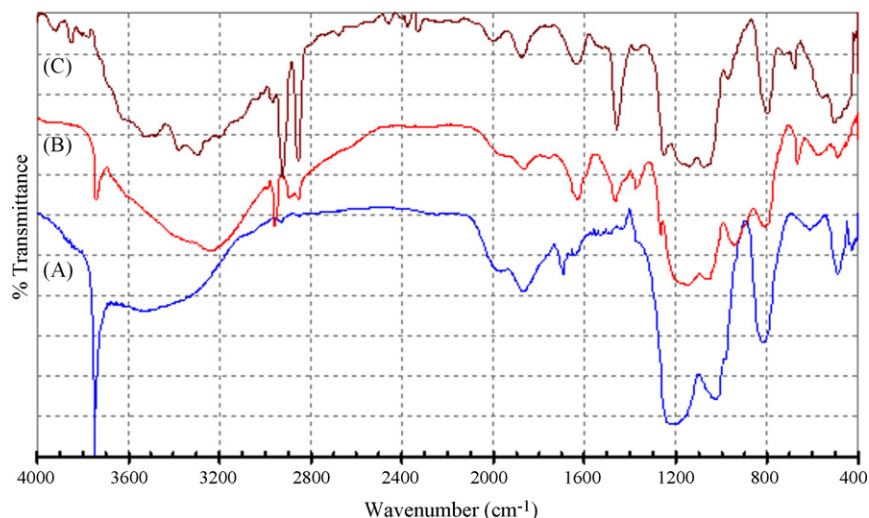
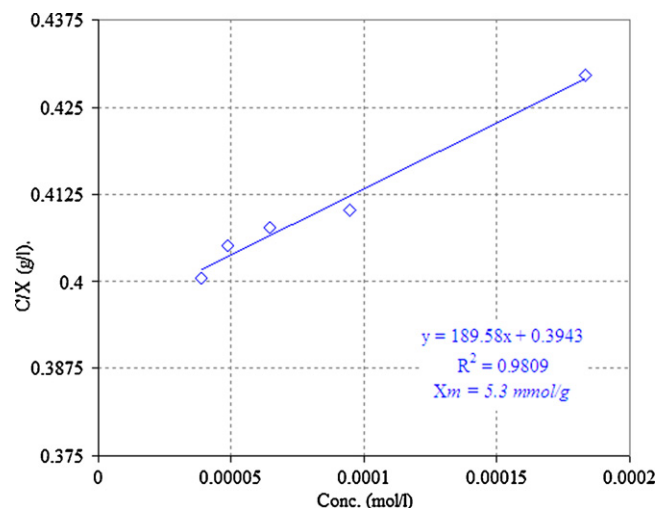


Fig. 8. Infrared spectra of OSU-6-W (curve A), OSU-6-W-GPTMS-1 (curve B), and OSU-6-W-GPTMS-2 (curve C).

**Table 2**  
Total coverage from three different determination methods.

Sample	Surface area (BET)	Spectrophotometric analysis (SA) (mmol/g)	Elemental analysis (EA)		<sup>29</sup> Si NMR			Total coverage (molecule/nm <sup>2</sup> )		
			C (%)	N (%)	Q <sup>2</sup> (%)	Q <sup>3</sup> (%)	Q <sup>4</sup> (%)	SA	EA	NMR
OSU-6-W	1283	...	0.10	0.06	13.89	71.73	14.38	...	...	...
OSU-6-W-GPTMS-1	966	3.88	17.36	0.08	0.00	49.32	50.68	2.42	2.09	1.99
OSU-6-W-GPTMS-2	720	4.50	22.24	0.11	0.00	30.77	69.23	3.76	3.53	3.17



**Fig. 9.** The Langmuir adsorption isotherms of Cu<sup>2+</sup> ions adsorbed by OSU-6-W-GPTMS-2 adsorbent.

### 3.4. Total surface loading of the glycidoxypropyl functional groups

The amount of glycidoxypropyl functional groups deposited on the surface was quantitatively determined using two variables. The surface loading ( $l$ ) expresses the amount of deposited molecules in mmol/g. The number of molecules deposited per nm<sup>2</sup> is given by the surface coverage ( $C$ ). Both values use the mass of the pure mesoporous silica before modification as a reference.

There is a broad range of analytical techniques available for the quantitative determination of the glycidoxypropyl functional groups (oxirane functions) [24]. In the case of surface-bonded groups, a decrease in reactivity had to be expected and, therefore, the most efficient procedures were selected after testing several possibilities found in the literature [24].

All three methods (Table 2) show that OSU-6-W-GPTMS-1 modified sample has an average coverage of 2.2 GPTMS molecules/100 Å<sup>2</sup>, while the OSU-6-W-GPTMS-2 sample has an average coverage of 3.5 GPTMS molecules/100 Å<sup>2</sup>. Thus, a significantly large coverage of functional groups is obtained compare with the results in the literature (2.20 group/nm<sup>2</sup>) [25]. This difference probably arises from the difference in pore sizes, 51.1 Å vs 40.0 Å, respectively, the use of amine as catalyst, and the intermediate water treatment in the silylation process. The larger pores can avoid steric congestion of the silane molecules. The treatment with water induces full coverage with adsorbed water that allows the formation of hydroxyl silanes and facilitates the assembly and aggregation of the incoming silyl groups on the surface. Thus, in the presence of water, the silane molecules are attached beyond the density of isolated silanols.

### 3.5. Metal adsorption study

#### 3.5.1. Uptake capacity

The uptake capacity of the modified OSU-6-W-GPTMS-2 silica was investigated using different amount of adsorbants interacting with 100 ppm solution of copper ions at pH 6.0. The results are shown in Fig. 9. The maximum uptake, calculated from the Langmuir adsorption isotherms, was 5.3 mmol Cu<sup>2+</sup>/g (or 336.8 mg/g). The glycidyl concentration in the material is 3.09 mmol/g so the adsorption of copper is remarkably high with a ratio of 1.7 copper ions to each grafted 3-glycidylpropylsilyl group. This result might arise from coordination of copper ions by both the glycidyl oxygen and the siloxane and silanol groups produced in the grafting reac-



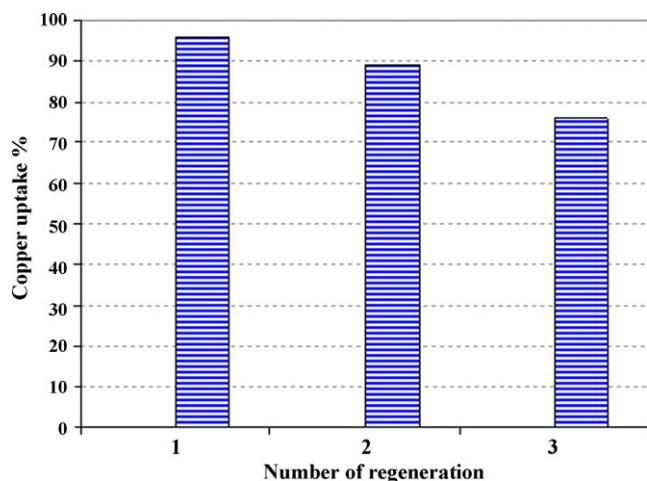


**Fig. 10.** The regeneration experiments of  $\text{Cu}^{2+}$  ions adsorbed by OSU-6-W-GPTMS-2 absorbent.

tion. Alternatively, ring opening of the glycidyl groups by water to produce pendant ethylene glycol groups could also generate additional Lewis base sites to coordinate copper ions. Additionally, there may also be metal-coordinating sites associated with the mesoporous silica framework. The good fit with the Langmuir isotherm model indicates that there are no major differences in the strength of adsorption of copper to any of the different sites that might be present. Whatever the cause, the extremely high capacity for copper adsorption makes this organically modified mesoporous silica an extremely promising reagent.

### 3.6. Regeneration of the absorbent

Treatment of the copper-loaded material with an aqueous solution of 2.0 M HCl three times each time stirring for 1 h resulted in the removal of the bound  $\text{Cu}^{2+}$  from the structure, regenerating the adsorbent for further metal ion uptake. The regenerated material (Fig. 10) shows a decrease in the copper ion uptake capacity reaching ~76% of the original capacity after the third regeneration. The decrease might be due to loss of the immobilized groups with washing or a strong interaction of the  $\text{Cu}^{2+}$  ions with the oxygen atoms causing it to not be released with HCl washing only. The latter, will lead to blocking the available sites for chelating. Overall, this material shows excellent regeneration.

## 4. Conclusion

The 3-glycidoxypropylsilyl moiety was readily introduced onto the surfaces of synthesized OSU-6-W mesoporous silica. Solid-state  $^{13}\text{C}$  and  $^{29}\text{Si}$  NMR and infrared spectroscopy, X-ray powder diffraction, and surface area measurements confirmed the successful derivatization. The derivatization methods employed showed a significantly high incorporation of organic groups onto the mesoporous silica. Mesoporous silica hybrids were obtained that had high surface areas and amounts of the active groups dispersed on the material. The inorganic-organic hybrid, OSU-6-W-GPTMS-2 had a very high copper(II) ion adsorption. These characteristics in physical, chemical and structural properties and in adsorptive behavior indicate that further studies on the catalytic abilities of new solids should be undertaken.

## Acknowledgements

The authors would like to acknowledge both OSU and KSU for their support to carry out this research work.

## References

- [1] P.K. Jal, S. Patel, B.K. Mishra, Chemical modification of silica surface by immobilization of functional groups for extractive concentration of metal ions, *Talanta* 62 (2004) 1005–1028.
- [2] A.G. Prado, L.A. Sales, R.M. Carvalho, J.C. Rubin, C. Airoldi, Immobilization of 5-amino-1,3,4-thiadiazole-thiol onto silica gel surface by heterogeneous and homogeneous routes, *J. Non-Cryst. Solids* 33 (2004) 61–67.
- [3] H.J. Im, E. Barnes, S. Dai, Z. Xue, Functionalized sol-gels for mercury(II) separation: a comparison of mesoporous materials prepared with and without surfactant templates, *Microporous Mesoporous Mater.* 70 (2004) 57–62.
- [4] Y. Lin, S. Fiskum, W. Yantase, H. Wu, S.W. Mattigod, E. Vorpapel, G.E. Fryxell, K.N. Raymond, J. Xu, Incorporation of hydroxypyridinone ligands into self-assembled monolayers on mesoporous supports for selective actinide sequestration, *Environ. Sci. Technol.* 39 (2005) 1332–1337.
- [5] P.M. Price, J.H. Clark, D.J. Macquarrie, Modified silicas for clean technology, *J. Chem. Soc. Dalton Trans.* 2 (2000) 101–110.
- [6] A. Stein, B. Melde, R. Schrodin, Hybrid inorganic-organic mesoporous silicates-nanoscale reactors coming of age, *Adv. Mater.* 12 (2000) 1403–1419.
- [7] D. Lindsay, D. Sherrington, J. Greig, R. Hancock, Novel chelating resins with remarkably high selectivities for copper(II) over zinc(II) ions, *J. Chem. Soc. Chem. Commun.* 17 (1987) 1270–1272.
- [8] P.D. Verweij, J.S.N. Van der Geest, W.L. Driessen, J. Reedijk, D.C. Sherrington, uptake by a novel benzimidazole ligand immobilized onto poly(glycidyl methacrylate-co-ethylene glycol dimethacrylate), *React. Polym.* 18 (1992) 191–201.
- [9] B.D. Moore, D.C. Sherrington, A. Zitsmanis, Conversion of a glycidyl methacrylate resin into a thirane analogue and subsequent immobilization of aliphatic amine and azole ligands, *J. Mater. Chem.* 2 (1992) 1231–1236.
- [10] A. Tuel, S. Gontier, Synthesis and characterization of trivalent metal containing mesoporous silicas obtained by a neutral templating route, *Chem. Mater.* 8 (1996) 114.
- [11] Houben-Weil Methoden der Organischen Chemie, Band VI/1a, Georg Thieme Stuttgart, 1979, pp. 357–382.
- [12] E. Pfannkoch, K.C. Lu, F.E. Regnier, H.G. Barth, Characterization of some commercial high performance size-exclusion chromatography columns for water-soluble polymers, *J. Chromatogr. Sci.* 18 (1980) 430–441.
- [13] P. Roumeliotis, K.K. Unger, Assessment and optimization of system parameters in size exclusion separation of proteins on diol-modified silica columns, *J. Chromatogr.* 218 (1981) 535–546.
- [14] G.R. Bogart, D.E. Leyden, T.M. Wade, W. Schafer, P.W. Carr, Spectroscopic investigation of the hydrolysis of  $\gamma$ -glycidoxypropylsilane bound to silica surfaces, *J. Chromatogr.* 483 (1989) 209–219.
- [15] A.V. Krasnoslobodtsev, S.N. Smirnov, Effect of water on silanization of silica by trimethoxysilanes, *Langmuir* 18 (2002) 3181–3184.
- [16] C.T. Kresge, M.E. Leonowicz, W.J. Roth, J.C. Vartuli, J.S. Beck, Ordered mesoporous molecular sieves synthesized by a liquid-crystal template mechanism, *Nature* 359 (1992) 710–712.
- [17] R.H. Glaser, G.L. Wilkes, C.E. Bronnimann, Solid state silicon-29 NMR of TEOS-based multifunctional sol-gel materials, *J. Non-Cryst. Solids* 113 (1989) 73–87.
- [18] X.S. Zhao, G.Q. Lu, A.K. Whittaker, G.J. Millar, H.Y. Zhu, Comprehensive study of surface chemistry of MCM-41 using  $^{29}\text{Si}$  CP/MAS NMR, FTIR, pyridine-TPD, and TGA, *J. Phys. Chem. B* 101 (1997) 6525–6531.
- [19] M. Templin, U. Wiesner, H.W. Spiess, Multinuclear solid-state-NMR studies of hybrid organic-inorganic materials, *Adv. Mater.* 9 (1997) 814–817.
- [20] G. Socrates, *Infrared Characteristic Group Frequencies Tables and Charts*, second ed., Wiley, Chichester, 1994.
- [21] A. Jentys, N.H. Pham, H. Vinek, Nature of hydroxy groups in MCM-41, *J. Chem. Soc., Faraday Trans.* 92 (1996) 3287–3291.
- [22] W. Lwowski, *Comprehensive Heterocyclic Chemistry*; Ed., Pergamon Press, Oxford, U.K., 1984; Vol. 7, p 99.
- [23] A.S. Piers, C.H. Rochester, IR studies of adhesion promoters. Part 3. Adsorption and coupling of bifunctional silanes on silica at the solid/liquid interface, *J. Chem. Soc., Faraday Trans.* 91 (1995) 1253–1260.
- [24] N.D. Cheronis, T.S. Ma, *Organic Functional Group Analysis by Micro and Semimicro Methods*, Wiley, New York, 1964.
- [25] P.G. Mingalyov, A.Y. Fadeev, Activated silica supports for preparation of chromatographic sorbents. A comparative study of silicas containing attached epoxy, tosyloxy and halogen groups, *J. Chromatogr. A* 719 (1996) 291–297.